

Composite Modeling and Analysis of FDM Prototypes for Design and Fabrication of Functionally Graded Parts

Longmei Li, Q. Sun, C. Bellehumeur¹, and P. Gu²

Department of Mechanical and Manufacturing Engineering

¹Department of Chemical and Petroleum Engineering

The University of Calgary, Calgary, Alberta, T2N 1N4, CANADA

Abstract

Solid Freeform Fabrication technologies have potential to manufacture parts with locally controlled properties (LCP), which would allow concurrent design of part's geometry and desired properties. To a certain extent, Fused Deposition Modelling (FDM) has the ability to fabricate parts with LCP by changing deposition density and deposition orientation. To fully exploit this potential, this paper reports a study on the mechanical properties of FDM prototypes, and related materials and fabrication process issues. Both theoretical and experimental analyses of mechanical properties of FDM parts were carried out. To establish the constitutive models, a set of equations is proposed to determine the elastic constants of FDM prototypes. An example is provided to illustrate the model with LCP using FDM.

Key words: Fused Deposition Modeling, Composite Mechanics, Locally Controlled Properties.

1. Introduction

With recent advances in Solid Freeform Fabrication (SFF) technologies, it is possible to use these technologies to produce parts with desired mechanical properties. The ability to fabricate parts with locally controlled properties (LCP) would create opportunities for manufacturing of a whole new class of parts with graded compositions [Jackson *et al.*, 99] and [Cho *et al.*, 01]. Fused Deposition Modeling (FDM) has the potential to produce parts with LCP by changing deposition density and deposition orientation. A few examples with LCP are shown in Figure 1 b), c), d), e).

FDM processes fabricate prototypes by extruding a semi-molten filament through a heated nozzle in a prescribed pattern onto a platform layer by layer, as in shown Figure 1 a). After the semi-molten material is deposited onto the worktable it begins to cool and bond to the neighboring material diffusely. The bonding between the individual roads of the same layer and of neighboring layers is driven by the thermal energy of semi-molten material. FDM processes use several types of materials, such as Acrylonitrile-butadiene-styrene (ABS) and wax, to build conceptual and/or functional prototypes.

Most of the existing research work in FDM is primarily directed towards the development of new materials or techniques for material deposition [Agarwala *et al.*, 96] [Gray IV *et al.*, 98], [Yardimci *et al.*, 96]. The mechanical properties of ABS filament and FDM parts were also investigated by researchers such as [Comb *et al.*, 94], [Kulkarni and Dutta, 99] and [Rodriguez Matas, 99].

ABS parts made by FDM processes essentially consist of partially bonded ABS filaments. Mechanical properties of FDM prototypes are governed by their meso-structures that are determined by manufacturing parameters. By selecting manufacturing parameters, such as deposition directions in layers and gap sizes between filaments, FDM processes can achieve LCP and produce prototypes with desired properties. To fully exploit this potential, issues concerning the mechanical properties of FDM parts and the fabrication process parameters, should be investigated. This paper describes a study on the mechanical properties of FDM prototypes.

²To whom all correspondences should be addressed: gu@enme.ucalgary.ca

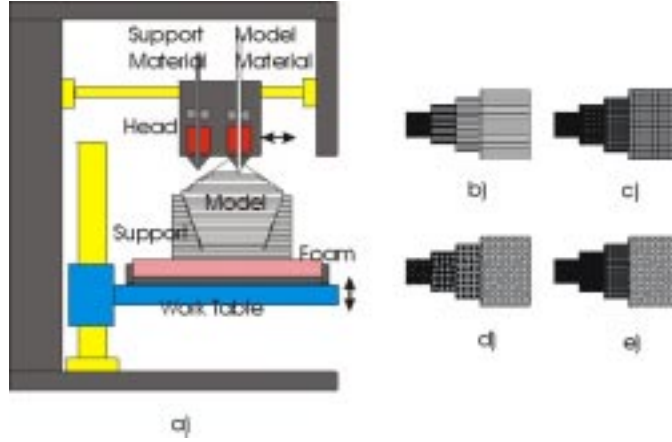


Figure 1: FDM process and the parts fabricated with graded mechanical properties

The remaining sections of this paper consist of the following parts: Section 2 is devoted to the modeling of the mechanical properties for design of FDM parts; experimental validation is given in Section 3. Section 4 provides an example of the prototypes with graded mechanical properties using LCP. The final section summarizes the main conclusions.

2. Modeling and Analysis of Mechanical Properties of FDM Prototypes

The FDM prototypes are orthotropic composites of ABS filaments, bonding between filaments and voids. They can be viewed and analyzed at different levels and on different scales. At macro level, they are studied as laminates of bonded laminars. At micro level, the properties of each lamina are functions of properties of filaments and void density.

2.1 Lamination Analysis of FDM Parts. To concurrently design mechanical geometries and properties, it is important to determine the effective stiffness so that the model can be used to predict the mechanical behaviors of the parts. Filament orientation θ is defined as the angle between the loading direction and longitudinal direction of filaments of each lamina. The in-plane constitutive relations for the case of *specialy orthotropic*, where $\theta = 0(or 90^\circ)$, the constitutive relation reduces to form of Equation 1:

$$\begin{bmatrix} \sigma_{11} \\ \sigma_{22} \\ \sigma_{12} \end{bmatrix} = \begin{bmatrix} Q_{11} & Q_{12} & 0 \\ Q_{12} & Q_{22} & 0 \\ 0 & 0 & Q_{66} \end{bmatrix} \begin{bmatrix} \epsilon_{11} \\ \epsilon_{22} \\ \epsilon_{12} \end{bmatrix}. \quad (1)$$

where $[\sigma_{ij}]$ and $[\epsilon_{ij}]$ are the in-plane stress and strain respectively. $[Q]$ is the stiffness matrix. Four independent elastic constants, namely, longitudinal Young's modulus E_{11} , transverse Young's modulus E_{22} , major Poisson's ratio ν_{12} , and shear Modulus G_{12} are required to describe the in-plane elastic behavior of a lamina. All elements in matrix $[Q]$ are functions of these constants. *General orthotropic* lamina refers to a lamina with fiber orientation other than 0° or 90° . Although, the stiffness matrix for general orthotropic lamina is fully populated with 6 elements. These six elements are functions of the four independent elements in matrix $[Q]$ [Mallick, 93].

A laminate is constructed by stacking a number of laminas in the thickness direction. The

overall properties can be modeled by the Lamination Theory [Mallick, 93]. As such, in macromechanical approaches, the stiffness matrix of a laminate is composed by properties of every lamina according to the Lamination Theory, while the in-plane elastic behavior of a unidirectional lamina may be fully described in terms of four elastic lamina properties including E_{11} , E_{22} , G_{12} and ν_{12} . For the design purpose, it is desirable to have reliable predictions of lamina properties as a function of constituent properties and geometric characteristics. One of the objectives of micromechanics is to obtain such relationships.

2.2 Micromechanics of Material with Voids. A variety of methods have been used to predict properties of composite materials as functions of constituent volume ratio and geometric packing parameters. Tsai [Tsai, 64] conducted an analysis based on variational principles in which contiguity of the fibers and fiber misalignment were considered. The filament contiguity was incorporated in theoretical prediction E_{22} , and the fiber misalignment was considered in E_{11} . The set of the equations, when being reduced to material with voids, is depicted below.

The longitudinal Young's modulus can be described by the equation:

$$E_{11} = k(1 - \rho_1)E \quad (2)$$

where E is the Young's modulus of the polymer, ρ_1 is the void density in Plane 1 (normal to the fibers), and k is an empirical factor that takes into account the fact that the filament may not be exactly parallel or perfectly straight. The prediction of transverse modulus, E_{22} , takes form:

$$E_{22} = (1 - C) \frac{[1 - (1 - \rho_1)\nu](1 - \rho_1)}{1 + 2\rho_1 - \nu(1 - 2\rho_1)} E \quad (3)$$

where ν is the Poisson's ratio of the polymer. The effective in-plane shear modulus, G_{12} , is given by:

$$G_{12} = (1 - C) \frac{1 - \rho_1}{1 + \rho_1} G \quad (4)$$

where G is shear moduli of the polymer. And the in-plane Poisson's ratio, ν_{12} , is given by the following relation:

$$\nu_{12} = (1 - C)\nu \quad (5)$$

Only the void density in the plane perpendicular to the fibers is required to compute the effective properties. The value of fiber contiguity factor C can be assigned to two extreme cases, (1) all filaments are isolated, $C = 0$; (2) all fibers are contiguous, $C = 1$. The effective Poisson's ratio, ν_{12} , is found to be the same as that of polymer when $C = 0$. It is the same as Hashin and Rosen's conclusion [Hashin and Rosen, 64].

Tsai's equations may be suitable for materials with cavities, but they could be used for FDM parts only under the assumption of perfect bonding among filaments. However, this assumption is not valid for the FDM process according to the ABS sintering experiments that were conducted in this research.

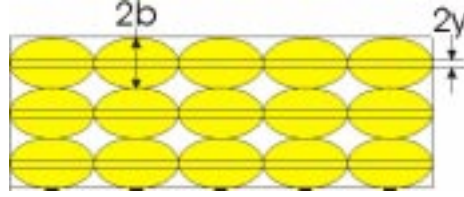


Figure 2: Fiber volume fraction in the transverse direction

2.3 Modeling of Elastic Constants for FDM Prototypes. The previous section demonstrated that FDM prototypes are composites of partially bonded ABS filaments and voids. Because of imperfect bonding, A new set of equations is proposed to calculate the elastic constants.

When loaded in longitudinal direction, a unidirectional FDM part is an aggregate of ABS filaments. Longitudinal Young's Modulus can be predicted well by the rule of mixtures. Therefore, Longitudinal Young's Modulus is:

$$E_{11} = (1 - \rho_1)E \quad (6)$$

where E is Young's Modulus of P400 filament, and ρ_1 is the area void density in the plane normal to filaments. In the case of transverse normal loading, the bonding among the filaments is the load carrier. The following equation is proposed for Transverse Modulus:

$$E_{22} = \zeta(1 - \rho_2)E \quad (7)$$

where ζ is an empirical factor that takes into account the bonding strength. ρ_2 is linear void fraction along the transverse direction. Refer to Figure 2, the definition of ρ_2 is:

$$\rho_2 = \frac{b - y}{b}. \quad (8)$$

Term $(1 - \rho_2)$ is the ratio of bonding length to overall dimensions. Similarly, the prediction of the in-plane shear modulus takes form:

$$G_{12} = \zeta(1 - \rho_2)G, \quad (9)$$

where G is the Shear Modulus of P400 filament, and the in-plane Poisson's ratio, ν_{12} , is same as that of ABS filaments, ν :

$$\nu_{12} = \nu \quad (10)$$

Comparing Equations 6 through 10 with Equations 2 to 5, the significant differences are in the predictions of E_{22} and G_{12} . Void density ρ_2 is introduced to count the potential load carrying dimension, whereas $\zeta(1 - \rho_1)$ results in the ratio of the effective load carrying media. Since the estimation of these elastic constants requires the void density in the plane perpendicular to filaments ρ_1 and bond length ratio ρ_2 , the calculations of the void densities are the topic of the next section.

2.4 Micro-scopic Images Analysis. Theoretical calculations of strength, modulus, and other properties for a FDM part are based on the the void densities ρ_1 and ρ_2 . Therefore the cross-sections of FDM specimens are studied under a microscope. Unidirectional cubic specimens of dimension $10 \times 8 \times 20mm$ were made with different gap sizes. They were cut in the middle plane

Table 1: Results of digitized image analysis

Gap Size(μm)	ρ_1	ρ_2
-50.0	0.0343	0.2776
-25.4	0.0434	0.3419
0	0.0799	0.4038
100	0.1990	1

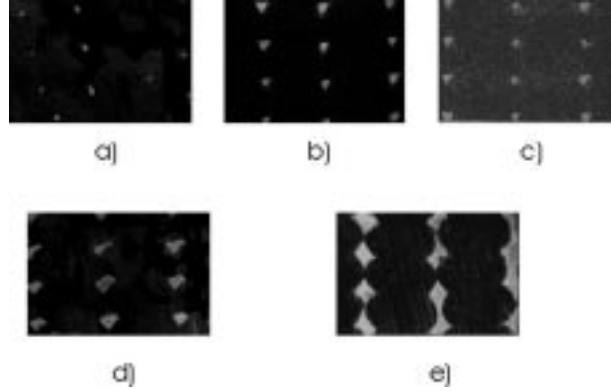


Figure 3: Meso-structures of different gap settings. a) $g = -0.100mm$; b) $g = -0.050mm$; c) $g = -0.0254mm$; d) $g = 0.0mm$ and e) $g = +0.100mm$

which is normal to filaments. Then the photos of meso-structures were taken under a microscope, as shown in Figure 3. They were analyzed by using image processing software. Void densities ρ_1 and ρ_2 were calculated, and the results are listed in Table 1. From the observation and the image analysis, it can be concluded that the voids appear periodically when the negative gap is small. When the negative gap reaches $-0.1mm$, the dimensional accuracy and surface quality of the specimen become very poor, and the periodicity can rarely be observed.

3. Experimental Validation

The theoretical stiffness model developed previously is a function of deposition densities and deposition orientations. To validate the model and method, the experimental analysis was carried out. The experiments tested the orthogonal-ply specimens, and the experimental results were compared with those of constitutive modeling described in Section 2. All specimens were manufactured by the FDM2000 machine. The elastic constants of P400 filaments were cited from work of Rodriguez Matas [Rodriguez Matas, 99], listed in Table 2, as the inputs of the theoretical calculations.

Table 2: Elastic Properties of P400 filament

Elastic Constant	Value
Young's Modulus, E	$2230 \pm 15MPa$
Shear Modulus, G	$833 \pm 7.6MPa$
ν	0.34 ± 0.02

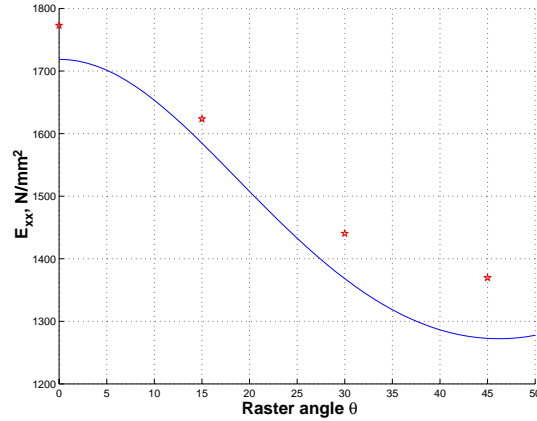


Figure 4: Young's modulus *vs* deposition Orientation in orthogonal-ply specimens

Table 3: Orthogonal-ply specimen test results

Specimen	Young's Modulus <i>MPa</i>		Difference
	Experimental	Theoretical	Percent
[0/90]	1772.9	1718.7	3.1
[15/-75]	1623.4	1584.7	2.4
[30/-60]	1440.4	1368.2	5.0
[45/-45]	1369.6	1272.7	7.1

The stiffness matrix of orthogonal-ply specimens can be constructed according to the procedure described in Section 2. As a result of the laminate modeling, the in-plane Young's modulus of the orthogonal-ply symmetric laminates with different $[\theta/(\theta - 90^\circ)]$ fiber orientations is a non-linear function of the deposition angle, as shown in Figure 4. It can be observed from the figure that the laminate with raster angles of approximately [45/-45] yields the minimum modulus of elasticity. The laminate with raster angles of [0/90] has the highest Young's Modulus. The experiments with the orthogonal-ply symmetric specimens were tested to determine the same in-plane moduli. The specimens with raster angles of [0/90], [30/-60], [45/-45], and [15/-75] were manufactured with the same thickness of 11 layers. These experimentally determined values were then compared with the theoretically predicted values to evaluate the effectiveness of the proposed laminate modeling approach, in Table 3 and marked as "*" in Figure 4. The experiment data were in good agreement with the results of laminate modeling.

4. Example

The purpose of the study of mechanical behaviors of FDM prototypes is to establish the models for design and fabrication of the parts with the desired mechanical properties through local composition control. This can be carried out with FDM process by changing deposition density and orientations to obtain the required properties.

The design of the example part with graded mechanical properties is shown in Figure 5a). Assume that the geometrical and functional constraints require the smaller section with equal or higher stiffness than that of the larger section areas. Therefore, the properties are gradient along

Table 4: Configuration of the axis

	l_1	l_2	l_3
Length(mm)	20	20	20
Deposition strategy ^o	[0/0]	[0/90]	[45/-45]
Gap (μm)	-25.4	-25.4	-25.4
E_{xx}^i	2137.7	1718.7	1272.7

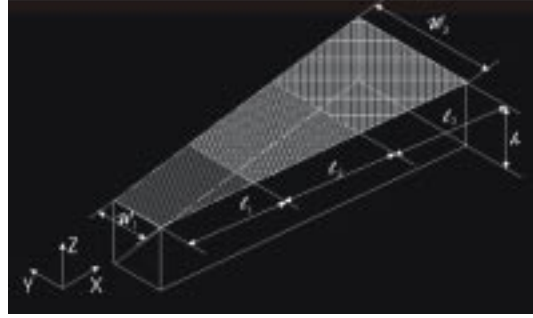


Figure 5: An axis with gradient property.

Axis X . Different deposition strategies and deposition densities were used for different sections of the part to meet the requirements as listed in Table 4. Young's modulus E_{xx} of each section calculated according to the stiffness modeling are listed in the table. If an external axial force P is applied at each end, the overall elongation ΔL is calculated using the following equation:

$$\Delta L = \sum_{i=1}^3 \int \frac{PL_i}{E_{xx}^i A_i(x)} dx. \quad (11)$$

where L_i is the length of each section, E_{xx}^i is the Young's Modulus of the section, and $A_i(x)$ is the cross-sectional area of the section. With locally controlled deposition density and deposition orientation, it is possible to make the section with smaller cross-sectional area as stiff as, or even stiffer than, the section with bigger cross-sectional area.

5. Concluding Remarks

The design and fabrication of products with LCP would make it possible to create a new class of products with desired mechanical and material characteristics. This paper reported a study on modeling of in-plane mechanical properties of FDM prototypes relating to fabrication parameters. Based on both the theoretical and the experimental analyses, a set of new equations of calculating the elastic constants were proposed and validated, which were used to determine the constitutive models of FDM parts. An example was presented to illustrate the design and fabrication of the FDM prototypes with required mechanical properties by locally controlled deposition density and orientations. Different deposition densities, angles and their combinations can be employed in producing the required stiffness properties of manufactured parts. The further study is currently underway in investigating void geometry and density with more manufacturing parameters.

Acknowledgements

The financial support for this research was provided by the National Sciences and Engineering Research Council of Canada (NSERC) through Research Grant OGP0192173. The authors would like to thank Brandon Ferguson and Art Moehrle for their assistance with experiments performed in the research.

References

- [Agarwala *et al.*, 96] M. K. Agarwala, A. Bandyopadhyay, R. van Weeren, N. A. Langrana, A. Safari, and S. C. Danforth, *Fused Deposition of Ceramics (FDC) for Structural Silicon Nitride Components*, Solid Freeform Fabrication Symposium, Austin, TX, Aug. 8th, 1996.
- [Gray IV *et al.*,98] Robert W. Gray IV, Donald G. Baird and Jan Helge Bohn, *Effects of processing conditions on short TLCP fiber reinforced FDM parts*, Rapid Prototyping Journal, Vol. 4, No. 1, pp. 14-25, 1998.
- [Cho *et al.*, 01] W. Cho, E. M. Sachs, N. M. Patrikalakis, M. Cima, T. R. Jackson, H. Liu, J. Serdy, C. C. Stratton, H. Wu, and R. Resnick, *Methods for Distributed Design and Fabrication of Parts with Local Composition Control*, Proceedings of the 2001 NSF Design and Manufacturing Grantees Conference, Tampa, FL, USA, January 2001.
- [Comb *et al.*, 94] Comb, J. W., Priedeman, W. R., and Turley, P. W., *Layered Manufacturing Control Parameters and Material Selection Criteria* Manufacturing Science and Engineering, PED-Vol. 68-2, Nov. 6-11, pp. 547-556, 1994.
- [Hashin and Rosen, 64] Zvi Hashin and B. Walter Rosen, *The Elastic Moduli of Fiber-Reinforced Materials*, Transactions of ASME: Journal of Applied Mechanics, Vol. 86, pp. 223-232, June 1964.
- [Jackson *et al.*, 99] T. R. Jackson, H. Liu, N. M. Patrikalakis, E. M. Sachs, and M. J. Cima. *Modeling and Designing Functionally Graded Material Components for Fabrication with Local Composition Control* Materials and Design, June 1999, Vol. 20, No. 2/3, pp. 63-75.
- [Kulkarni and Dutta, 99] P. Kulkarni and D. Dutta, *Deposition Strategies and Resulting Part Stiffnesses in Fused Deposition Modeling*, ASME Transactions: Journal of Manufacturing Science and Engineering, Vol. 121, pp. 93-103, February, 1999.
- [Mallick, 93] P. K. Mallick, *Fiber-reinforced Composites: materials, manufacturing, and design*, Second Edition, Marcel Dekker, Inc, 1993.
- [Rodriguez Matas, 99] Jose F. Rodriguez Matas, "Modeling the mechanical behavior of fused deposition acrylonitrile-butadiene styrene polymer components", Ph. D Dissertation, Department of Aerospace and Mechanical Engineering, Notre Dame, Indiana, 1999.
- [Tsai, 64] Stephen W. Tsai, *Structural Behavior of Composite Materials*, NASA CR71, 1964.
- [Yardimci *et al.*, 96] M. Atif Yardimci, S. I. Guceri, S. C. Danforth, and M. Agarwala, "Part Quality Prediction Tools for Fused Deposition Processing", Proceedings of the Solid Freeform Fabrication Symposium, Austin, TX, pp. 539-548, Aug. 1996.